Appl. Phys. B 38, 263–268 (1985)

Applied Physics B Photophysics and Laser Chemistry

Analysis of the Dispersion Relation of Nonlinear Slab-Guided Waves

Part II: Symmetrical Configuration

U. Langbein, F. Lederer, H.-E. Ponath, and U. Trutschel

Department of Physics, University of Jena, DDR-6900 Jena, German Democratic Republic

Received 14 May 1984/Accepted 18 January 1985

Abstract. The dispersion relations of TE-polarized nonlinear guided waves (NGWs) in a symmetrical slab configuration (linear slab embedded between two identical media with a Kerr nonlinearity) are investigated in detail. Among even and odd NGWs the waveguide can support also NGWs, revealing an asymmetrical field pattern. The excitation of these NGWs requires a minimum guided power flux indicating a bifurcation of the corresponding dispersion curves.

PACS: 42.82, 42.65 B

Waveguiding layers with nonlinear substrat and/or superstrat regions can support a new type of guided waves, i.e. nonlinear guided waves (NGWs) [1–4]. In part I of this paper [4] the dispersion relations of these NGWs, travelling along an asymmetrical slab configuration, have been investigated. The present paper deals with the symmetrical configuration where both the substrat and the superstrat region possess identical dielectric properties. Such symmetrical configurations have already been considered elsewhere [1, 2]. The investigations presented here are consequences of our analysis of general asymmetrical configurations in [4]. In this way we intend to provide some additional aspects to the current discussion concerning NGW properties.

The first section contains a summary of some fundamental properties of NGWs in a symmetrical configuration. In particular, a symmetry-breaking mechanism is pointed out leading to a distinction between the totally symmetrical and the broken symmetrical case. In the next two sections the different NGW types are introduced and their dispersion relations are investigated extensively.

Section 4 deals with the power flux supported by a NGW. The relation between this power flux and the NGW-propagation constants has been numerically calculated.

1. Fundamental Properties of NGWs in Symmetrical Configurations

We consider a nonlinear slab waveguide, according to Fig. 1, where the material relations as well as the characteristic transverse field pattern of a NGW are indicated. Our notation corresponds to that of [4]. Symmetrical configuration means

$$\bar{\varepsilon}_1 = \bar{\varepsilon}_3, \quad a_1 = a_3 = a, \tag{1}$$

which implies

$$\alpha_1 = \alpha_3 = (\beta^2 - \omega^2/c^2\bar{\varepsilon}_1)^{1/2}, \tag{2}$$

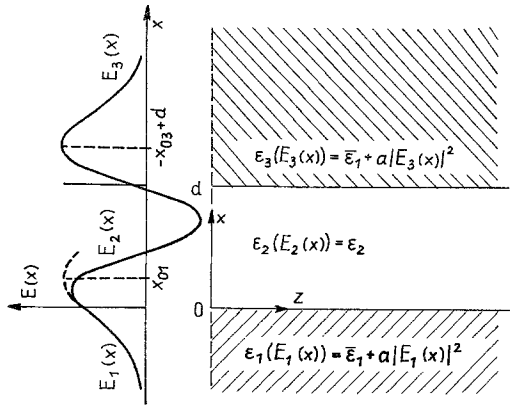

Fig. 1. Symmetrical waveguide configuration and characteristic field pattern $E(x)$ of a NGW

where β is the propagation constant. The symmetry condition (1) does not necessarily imply the equivalence of the effective dielectric coefficients

$$\varepsilon_{\varrho\mathrm{NL}} \equiv \bar{\varepsilon}_1 + \frac{a}{2} E_{(\varrho)}^2, \quad \varrho = 1, 3, \tag{3}$$

and of the related quantities

$$\alpha_{\varrho\mathrm{NL}} \equiv \alpha_1 \tanh(\alpha_1 x_{0\varrho}) = \pm(\beta^2 - \omega^2/c^2 \varepsilon_{\varrho\mathrm{NL}})^{1/2}, \quad \varrho = 1, 3, \tag{4}$$

as well. For that reason the dispersion relation

$$\tan\gamma_2 d = \frac{\gamma_2(\alpha_{1\mathrm{NL}} + \alpha_{3\mathrm{NL}})}{\gamma_2^2 - \alpha_{1\mathrm{NL}}\alpha_{3\mathrm{NL}}} \tag{5}$$

is formally the same as in [4].

$E_{(\varrho)}$, appearing in (3) is the NGW-field strength at the interfaces $x=0$ ($\varrho=1$) and $x=d$ ($\varrho=3$), respectively. $E_{(\varrho)}$ is related to the parameter $x_{0\varrho}$ determining the situation of the evanescent field maxima with respect to the corresponding interfaces

$$E_{(\varrho)} = \pm(2/a)^{1/2} \alpha_1 c/\omega (\cosh \alpha_1 x_{0\varrho})^{-1}, \quad \varrho = 1, 3. \tag{6}$$

We recall that $x_{0\varrho} > 0$ designates a virtual evanescent field maximum and $x_{0\varrho} < 0$ a real one. A virtual maximum is situated within the slab region where the nonlinear evanescent field solution does not apply (x_{01} in Fig. 1).

With respect to both interfaces the parameters introduced by (3), (4), and (6) are not independent of one another. Their mutual dependence is expressed by [Ref. 1, Eq. (15)] which simplifies for our symmetrical configuration to

$$\varepsilon_{1\mathrm{NL}} = \varepsilon_{3\mathrm{NL}}; \quad a/2E_{(1)}^2 = a/2E_{(3)}^2 \tag{7a}$$

and

$$\varepsilon_{1\mathrm{NL}} + \varepsilon_{3\mathrm{NL}} = \bar{\varepsilon}_1 + \varepsilon_2; \quad a/2(E_{(1)}^2 + E_{(3)}^2) = \varepsilon_2 - \bar{\varepsilon}_1. \tag{7b}$$

Both relations are valid within the ranges

$$\bar{\varepsilon}_1 \leqq \varepsilon_{\varrho\mathrm{NL}} \leqq \varepsilon_2, \quad 0 \leqq a/2E_{(\varrho)}^2 \leqq \varepsilon_2 - \bar{\varepsilon}_1 \tag{8}$$

only.

Relation (7a) represents the totally symmetrical case, where the symmetrical choice of the material parameters is also reflected by the effective dielectric coefficients $\varepsilon_{\varrho\mathrm{NL}}$, see dotted line in Fig. 2, and the field pattern as well. If this case applies the waveguide will support NGWs with even or odd symmetry of their transverse field pattern $E(x)$, see next section.

According to (7b) NGWs with an asymmetrical field pattern (a-NGWs) are also permitted for a symmetrical nonlinear waveguide. This remarkable symmetry-breaking mechanism of symmetrical nonlinear waveguides was first mentioned by Achmedijev [2].

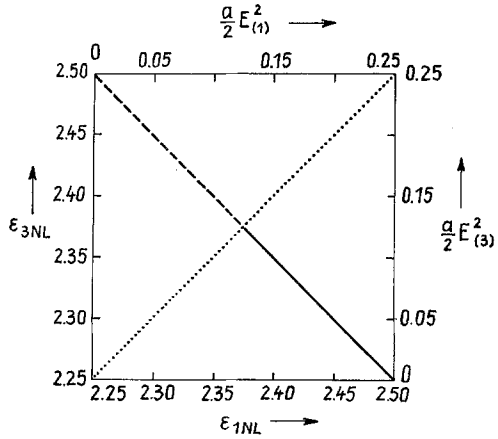

Fig. 2. Mutual dependence of $\varepsilon_{1\mathrm{NL}}$ and $\varepsilon_{3\mathrm{NL}}$ according to (7a) (dotted line) and (7b) (broken line for $\varepsilon_{1\mathrm{NL}} < \varepsilon_{3\mathrm{NL}}$, solid line for $\varepsilon_{1\mathrm{NL}} > \varepsilon_{3\mathrm{NL}}$); $\bar{\varepsilon}_1 = \bar{\varepsilon}_3 = 2.25$; $\varepsilon_2 = 2.50$

The second diagonal in Fig. 2 illustrates relation (7b).

The solid line applies for $\varepsilon_{1\mathrm{NL}} > \varepsilon_{3\mathrm{NL}}$ ($E_{01}^2 > E_{03}^2$), the broken line is valid for $\varepsilon_{3\mathrm{NL}} > \varepsilon_{1\mathrm{NL}}$ ($E_{03}^2 > E_{01}^2$). At the intersection point of both diagonals in Fig. 2

$$\varepsilon_{1\mathrm{NL}} = \varepsilon_{3\mathrm{NL}} = \frac{\bar{\varepsilon}_1 + \varepsilon_2}{2}, \quad a/2E_{(1)}^2 = a/2E_{(3)}^2 = 1/2(\varepsilon_2 - \bar{\varepsilon}_1) \tag{9}$$

both cases (7a) and 7b) coincide.

2. The Totally Symmetrical Case

In this case $\alpha_{1\mathrm{NL}} = \alpha_{3\mathrm{NL}}$ holds and the general NGW-dispersion relation (5) splits into two parts

$$\tan(\gamma_2 d) = \alpha_{1\mathrm{NL}}/\gamma_2, \tag{10}$$

$$\cot(\gamma_2 d) = -\alpha_{1\mathrm{NL}}/\gamma_2, \tag{11}$$

where

$$\gamma_2 = (\omega^2/c^2 \varepsilon_2 - \beta^2)^{1/2}, \tag{12a}$$

$$\omega^2/c^2 \varepsilon_{1\mathrm{NL}} < \beta^2 \leqq \omega^2/c^2 \varepsilon_2. \tag{12b}$$

Equation (10) represents the dispersion relation for even NGWs (e-NGW); (11) is the dispersion relation for odd NGWs (o-NGW). The corresponding field pattern can be easily derived from [Ref. 1, Eq. (7)] using (7a), (10) or (11), respectively

$$E_3(x) = \pm E_{(1)}[\cosh \alpha_1 (x-d) + \alpha_{1\mathrm{NL}}/\alpha_1 \sinh \alpha_1 (x-d)]^{-1}, \tag{13a}$$

$$E_2(x) = E_{(1)} \frac{\begin{matrix}\cos \\ \sin\end{matrix} \{\gamma_2(d/2 - x)\}}{\begin{matrix}\cos \\ \sin\end{matrix} \{\gamma_2 d/2\}}, \tag{13b}$$

$$E_1(x) = E_{(1)}[\cosh \alpha_1 x - \alpha_{1\mathrm{NL}}/\alpha_1 \sinh \alpha_1 x]^{-1}. \tag{13c}$$

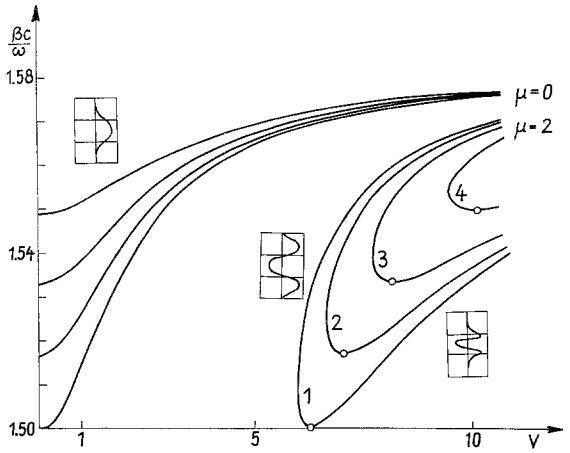

Fig. 3. Dispersion curves for two low-order e-NGWs. Fixed parameters: $\bar{\varepsilon}_1=\bar{\varepsilon}_3=2.25$; $\varepsilon_2=2.50$. Varied parameters: $\varepsilon_{1\,\mathrm{NL}}$: 2.2501(1); 2.30(2); 2.35(3); 2.40(4). The associated field pattern are schematically drawn

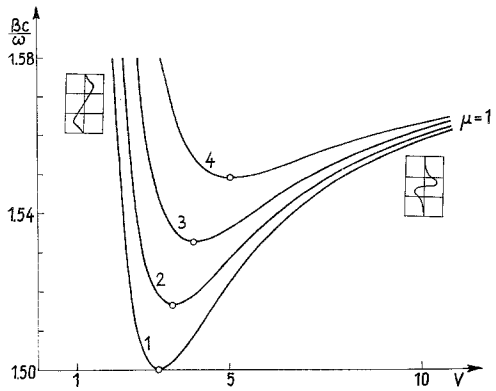

Fig. 4. Lowest-order dispersion curves for o-NGWs; notation and parameters as in Fig. 3

The upper sign in (13a) and the cos-function in (13b) are valid for the e-NGWs; the other ones hold for o-NGWs. The symmetry-plane is $x=d/2$. Due to $\varepsilon_{1\,\mathrm{NL}}=\varepsilon_{3\,\mathrm{NL}}$, (6a), both NGW-families introduces in [4] coincide. There is no longer an invariant evanescent-field maximum with respect to one slab interface. Every change in the situation of both evanescent field maxima takes place simultaneously.

2.1. Even NGWs

Figure 3 shows the dispersion curves of two low-order e-NGWs. The curves are solutions of (10) and illustrate the β-dependence on the film parameter $V=\omega/cd(\varepsilon_2-\bar{\varepsilon}_1)^{1/2}$. The effective dielectric constant $\varepsilon_{1\,\mathrm{NL}}$ is varied. Curves with common numbers belong to the same $\varepsilon_{1\,\mathrm{NL}}$ determining the lower β-limit, see (12b). The transition points, where the evanescent field maxima cross the slab interfaces, are indicated by small circles. Their situation in the V-scale is given by [Ref. 1, Eqs. (18) and (19)] which simplify to

$$V_\mu^{(T)}=\mu\pi\,[(\varepsilon_2-\bar{\varepsilon}_1)/(\varepsilon_2-\varepsilon_{1\,\mathrm{NL}})]^{1/2},\qquad \mu=0,2,4,\ldots, \tag{14}$$

in the totally symmetrical case.

The lowest order waves $\mu=0$ terminate at $V_\mu^{(T)}=0$, i.e. they reveal a zero cut-off like in linear waveguide optics. The dispersion curve for $\varepsilon_{1\,\mathrm{NL}}=\varepsilon_2$ is given by $\beta=\omega/c\varepsilon_2^{1/2}$. This horizontal line represents the common asymptotic limit ($V\to\infty$) for all other dispersion curves at the same time.

2.2. Odd NGWs

The dispersion curves for o-NGWs are similar to those of the e-NGWs. Their transition points are also determined by (14) but for $\mu=1,3,5\ldots$. Only the lowest-order wave $\mu=1$ plays an extraordinary role. Some dispersion curves of this wave are shown in Fig. 4. These curves do not turn back to $V\to\infty$ after having passed their transition points but acquire the upper β-limit for finite V-values

$$V=V_1^{\mathrm{odd}}=2[(\varepsilon_2-\bar{\varepsilon}_1)/(\varepsilon_2-\varepsilon_{1\,\mathrm{NL}})]^{1/2}. \tag{15a}$$

An o-NGW driven at this limit reveals the same dispersion relation

$$\beta^2=\omega^2/c^2\varepsilon_2 \tag{15b}$$

like a plane wave travelling in the unbounded slab material. For that reason we call it "pseudo-bulk wave". Beyond the limit (15b), i.e. for $\beta^2>\omega^2/c^2\varepsilon_2$, the sine-function in the inner field solution (13b) transfers into a sinh-function since γ_2 becomes imaginary. The resulting NGW is known as "nonlinear surface polariton" [1, 2] not to be treated in this paper. In this respect the pseudo-bulk wave represents an intermediate state between a lowest-order o-NGW and a nonlinear surface polariton. The corresponding intermediate field pattern $E_2(x)$ in the slab region is a strictly linear one; proceed $\gamma_2\to 0$ in (13b).

3. The Broken Symmetrical Case

In this case (7b) holds, indicating the existence of an asymmetrical field pattern. Since our symmetrical geometry leads to field equations that are invariant to the coordinate transformation $x\to-(x-d)$, every a-NGW is degenerated. A given a-NGW has a counterpart with a mirror-symmetric field pattern but with the same propagation constant β. This β-degeneration is also reflected by the invariance of the dispersion relation (5) and (7b) with respect to an exchange $\varepsilon_{1\,\mathrm{NL}}\leftrightarrow\varepsilon_{3\,\mathrm{NL}}$. Consequently, we can restrict ourselves

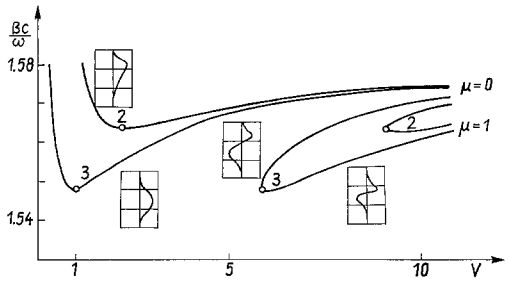

Fig. 5. Dispersion curves for a-NGWs belonging to Family A; notation and parameters as in Fig. 3

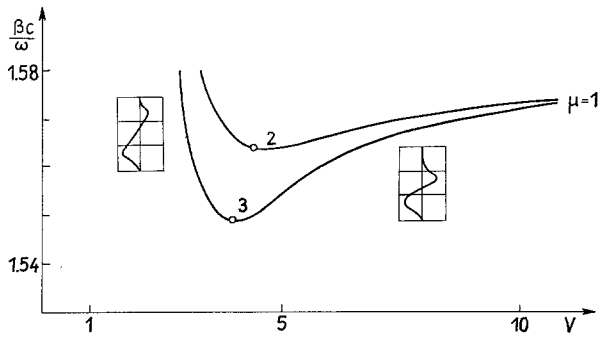

Fig. 6. Same type of dispersion curves as in Fig. 5 but for NGW Family B

to a-NGWs which belong to the broken half-diagonal in Fig. 2, i.e. to $\varepsilon_{3\mathrm{NL}} > \varepsilon_{1\mathrm{NL}}$. The solid half diagonal belongs to a-NGWs with the same dispersion relation but with mirror-symmetric field pattern.

Figures 5 and 6 show numerical solutions of the dispersion relation (5) of the type $\beta(V)$. Only the interesting low-order a-NGWs are indicated. Due to (4) and (7b) the permitted β-range is given by

$$\omega^2/c^2\varepsilon_{\mathrm{NL}}^{(+)} \leqq \beta^2 \leqq \omega^2/c^2\varepsilon_2\,, \tag{16}$$

where

$$\varepsilon_{\mathrm{NL}}^{(+)} = \operatorname*{Max}_{\varrho=1,3} \varepsilon_{\varrho\mathrm{NL}} \geqq 1/2(\bar{\varepsilon}_1 + \varepsilon_2)\,. \tag{17}$$

Figure 5 illustrates the dispersion curves for two members of Family A. These a-NGWs reveal an invariant virtual evanescent field maximum, see [4] for details.

In contrast to the asymmetrical configuration [Ref. 1, Fig. 3] the set of curves for a-NGWs with an invariant evanescent field maximum above the slab region coincides with the corresponding set for a-NGWs with an invariant field maximum below the slab region. The pseudo-bulk limit, determined by [Ref. 1, Eq. (22)] of the lowest-order wave is clearly seen.

Figure 6 belongs to the lowest-order members of Family B which reveal an invariant real evanescent field maximum above or below the slab region. All transition points are determined by [Ref. 1, Eqs. (18)–(20)].

4. The Power Flux Supported by a NGW

The power flux P^{NL} perpendicular through a stripe of unit width (with respect to the y-coordinate) in an asymmetrical configuration was derived in [4]. In the totally symmetrical case [Ref. 1, Eqs. (24) and (25)] modify to

$$P^{\mathrm{NL}} = P_0(\varepsilon_{1\mathrm{NL}} - \bar{\varepsilon}_1)\beta \cdot \left[d_{\mathrm{eff}}^{\mathrm{NL}}(1 + \alpha_{1\mathrm{NL}}^2/\gamma_2^2) + \frac{2\alpha_{1\mathrm{NL}}(\alpha_1 - \alpha_{1\mathrm{NL}})}{\gamma_2^2(\alpha_1 + \alpha_{1\mathrm{NL}})} \right], \tag{18a}$$

where

$$d_{\mathrm{eff}}^{\mathrm{NL}} = d + \frac{4}{\alpha_1 + \alpha_{1\mathrm{NL}}} \tag{19a}$$

and

$$P_0 = 1/4\mu_0\omega \cdot 2/a \tag{20}$$

denote an effective slab thickness and a normalization constant, respectively.

The broken symmetrical case provides instead of (18a) and (19a)

$$P^{\mathrm{NL}} = P_0(\varepsilon_{1\mathrm{NL}} - \bar{\varepsilon}_1)\beta \cdot \left[d_{\mathrm{eff}}^{\mathrm{NL}}(1 + \alpha_{1\mathrm{NL}}^2/\gamma_2^2) + \frac{\alpha_{1\mathrm{NL}}(\alpha_1 - \alpha_{1\mathrm{NL}})}{\gamma_2^2(\alpha_1 + \alpha_{1\mathrm{NL}})} \right. \tag{18b}$$

$$\left. + \frac{(\varepsilon_2 - \varepsilon_{1\mathrm{NL}})\alpha_{3\mathrm{NL}}(\alpha_1 - \alpha_{3\mathrm{NL}})}{(\varepsilon_2 - \varepsilon_{3\mathrm{NL}})\gamma_2^2(\alpha_1 + \alpha_{3\mathrm{NL}})} \right], \tag{19b}$$

$$d_{\mathrm{eff}}^{\mathrm{NL}} = d + 2/(\alpha_1 + \alpha_{1\mathrm{NL}}) + 2/(\alpha_1 + \alpha_{3\mathrm{NL}})\,. \tag{19b}$$

Equations (18)–(20), (7b) and the appropriate dispersion relations (5), (10), (11) have been used to illustrate, in Figs. 7 and 8, the relation between P^{NL} and our crucial parameter $a/2E_{(1)}^2$ for fixed film parameters V. In Fig. 7 $V=4$ is assumed where only the lowest-order

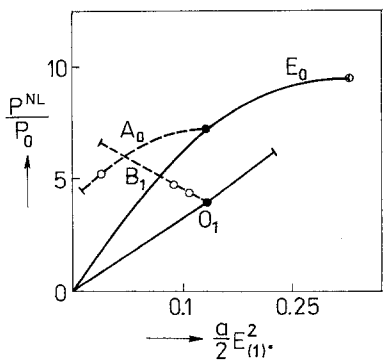

Fig. 7. Mutual dependence between the field strength at the boundary $x=0$; $a/2E_{(1)}^2$ and the normalized power flux P^{NL}/P_0 for a given film parameter $V=4$, $\bar{\varepsilon}_1$, ε_2 as in Fig. 2; E: e-NWG, O: o-NGW, A, B: a-NGW of Family A and B, respectively; the subscribed numbers designate the wave number μ; small circles, spots, squares, and lines indicate transition, bifurcation, family transition, and pseudo-bulk limit points, respectively

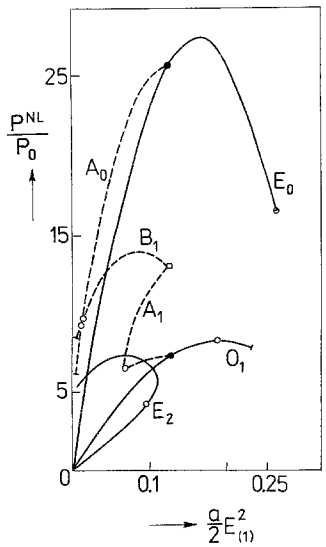

Fig. 8. Same type of curves as in Fig. 7 but for $V=8$

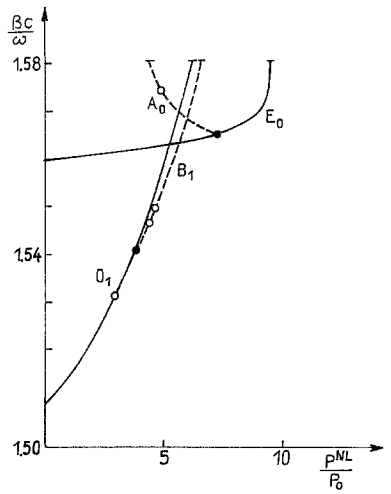

Fig. 9. Effect of the normalized power flux P^{NL}/P_0 on the propagation constant β for a fixed film parameter $V=4$; notation and parameters as in Fig. 8

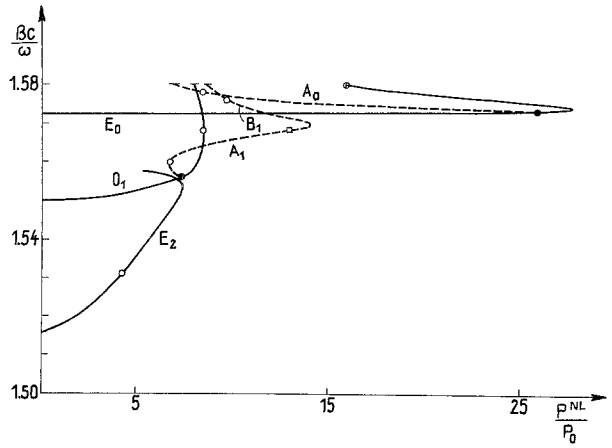

Fig. 10. Same type of curve as in Fig. 9 but for $V=8$

NGWs of every type can be excited, see Figs. 3–6. The dark spots indicate bifurcation points where the a-NGW-curves (broken lines) branch off from the e-NGW and o-NGW curves, respectively. The common $a/2E^2_{(1)}$-coordinate of these points is determined by (9). All curves terminate at their pseudo-bulk limit. The degeneration of a-NGWs gives rise to a second pair of (broken) curves starting also at the bifurcation points. Since these curves are mirror-symmetric to the indicated ones with respect to the symmetry line (9), they have been omitted for the sake of clearness. The small circles at the a-NGWs designate transition points. In contrast to the single interface configuration used by Kaplan [5] these points do not play an extraordinary role. In particular, they do not provide any information concerning the stability of the NGWs under consideration, as it was assumed in [6].

In Fig. 8 $V=8$ is assumed permitting the excitation of some additional NGWs. All features, discussed for Fig. 7, appear again. The small square designates a "family transition point", where the a-NGW ($\mu=1$) changes from Family A to Family B. The $a/2E^2_{(1)}$ coordinate of this point is also given by (9). Additionally, the e-NGW-curve ($\mu=2$) appears.

Up to now $\varepsilon_{1\,NL}$ (or $a/2E^2_{(1)}$) played the role of the crucial parameter in describing the effct of the nonlinearity in our waveguide configuration. This parameter was useful in the interpretation of the new formulas. It permitted also a comparison with the familiar linear waveguide problem. On the other hand, there is no reason to prefer a parameter which is associated with a single interface in a slab configuration. Eventually, the question arises which parameter(s) can be controlled in a definite experiment. In this connection, the power flux supported by a NGW appears to be at least a more physical quantity than $\varepsilon_{1\,NL}$. The replacement of $\varepsilon_{1\,NL}$ by P^{NL} to be the primary nonlinear parameter was performed numerically in Figs. 9 and 10, where the effect of P^{NL} on the propagation constant is illustrated. Generally, the same features like in Figs. 7 and 8 can be stated. Note that the broken curves are valid for both degenerated a-NGWs, the field pattern of them are mutually mirror-symmetric. The limiting case of the linear waveguide is covered by $P^{NL}=0$. The agreement with Achmedijev's results is obvious. In [2] the inverse relation $P^{NL}(\beta)$ was calculated. The corresponding analytical relation can be derived from (18a) and (18b) by substituting $\alpha_{1\,NL}$ with the help of the appropriate dispersion relations.

5. Conclusions

The symmetrical nonlinear slab configuration permits TE-polarized even, odd and asymmetrical NGW so-

lutions being subject to different dispersion relations. The a-NGWs are degenerated. They form pairs the members of which reveal a common propagation constant but mirror-symmetric field pattern. The a-NGWs can be excited above a certain P^{NL}-threshold only. This threshold indicates bifurcation points in the $\beta(P^{NL})$ diagram where the a-NGW curves branch off from the e- or o-NGW curves, respectively. The e/o-NGW curves start at $P^{NL}=0$ implying vanishing nonlinearity. The $\beta(V)$-dispersion curves reveal a zero cut-off for the lowest-order e-NGWs. The lowest-order members of the remaining NGW types terminate at their pseudo-bulk limit, which indicates the transition from NGW solutions to nonlinear surface polaritons.

References

1. A.A. Maradudin: Second Int. School on Condensed Matter Physics, Varna, Bulgaria (1982)
2. N.N. Achmedijev: Zh. Eksp. Teor. Fiz. **83**, 545 (1982)
3. F. Lederer, U. Langbein, H.-E. Ponath: Appl. Phys. B **31**, 69 (1983)
4. U. Langbein, F. Lederer, H.-E. Ponath, U. Trutschel: Appl. Phys. B (to be published)
5. A.E. Kaplan: Sov. Phys. JETP **45**, 896 (1977)
6. D.J. Robbins: Opt. Commun. **47**, 309 (1983)

Responsible for Advertisements: E. Lückermann, G. Probst, Heidelberger Platz 3, D-1000 Berlin 33, Tel. (0 30) 82 07-1, Telex 01-85411
Responsible for the Text: H. K. V. Lotsch, Tiergartenstrasse 17, D-6900 Heidelberg. Printers: Brühlsche Universitätsdruckerei, Giessen, Printed in Germany
Springer-Verlag GmbH & Co. KG, D-1000 Berlin 33